BIOCHEMISTRY
including biophysical chemistry & molecular biology
Article

Biochemistry **2010,** *49,* 4921–4929 4921
DOI: 10.1021/bi100244j

Kinetic Mechanistic Studies of Cdk5/p25-Catalyzed H1P Phosphorylation: Metal Effect and Solvent Kinetic Isotope Effect

Min Liu,*,‡ Eleni Girma,‡ Marcie A. Glicksman,‡ and Ross L. Stein§

‡*Laboratory for Drug Discovery in Neurodegeneration, Harvard NeuroDiscovery Center, 65 Landsdowne Street, Fourth Floor, Cambridge, Massachusetts 02139, and* §*Sirtris Pharmaceuticals, Cambridge, Massachusetts 02139*

Received February 17, 2010; Revised Manuscript Received May 13, 2010

ABSTRACT: Cdk5/p25 is a member of the cyclin-dependent, Ser/Thr kinase family and has been identified as one of the principle Alzheimer's disease-associated kinases that promote the formation of hyperphosphorylated tau, the major component of neurofibrillary tangles. We and others have been developing inhibitors of cdk5/p25 as possible therapeutic agents for Alzheimer's disease (AD). In support of these efforts, we examine the metal effect and solvent kinetic isotope effect on cdk5/p25-catalyzed H1P (a histone H-1-derived peptide) phosphorylation. Here, we report that a second Mg^{2+} in addition to the one forming the MgATP complex is required to bind to cdk5/p25 for its catalytic activity. It activates cdk5/p25 by demonstrating an increase in k_{cat} and induces a conformational change that favors ATP binding but has no effect on the binding affinity for the H1P peptide substrate. The binding of the second Mg^{2+} does not change the binding order of substrates. The reaction follows the same rapid equilibrium random mechanism in the presence or absence of the second Mg^{2+} as evidenced by initial velocity analysis and substrate analogue and product inhibition studies. A linear proton inventory with a normal SKIE of 2.0 ± 0.1 in the presence of the second Mg^{2+} was revealed and suggested a single proton transfer in the rate-limiting phosphoryl transfer step. The pH profile revealed a residue with a pK_a of 6.5 that is most likely the general acid−base catalyst facilitating the proton transfer.

One of the pathological hallmarks of Alzheimer's disease (AD)[1] (*1*, *2*) is neurofibrillary tangles (NFTs). The major component of NFTs is hyperphosphorylated tau, the microtubule-associated protein (*3*). cdk5/p25 has been identified as one of the principle AD-associated kinases because of the increased activity of cdk5/p25 in the AD brain and its ability to phosphorylate tau at multiple sites (*4*−*6*). cdk5/p25 is a proline-directed Ser/Thr kinase and a member of the cyclin-dependent kinase family involved in cell cycle regulation. Unlike other members of the family that require association with a cyclin for activity, cdk5 associates with the activator protein p35. The resultant complex, cdk5/p25, of the neuronal-specific processing of p35 to p25 by calpain likely plays a role in the pathogenesis of AD (*5*−*7*).

With our understanding of the role of cdk5/p25 in the AD brain, the discovery and design of inhibitors of this enzyme have become a goal in the search for drugs for the treatment of AD. Understanding the mechanism of cdk5/p25 is critical for the design of inhibitors. We previously reported a random kinetic mechanism for cdk5/p25 catalysis (*8*). In this article, we reveal additional features of cdk5/p25 catalysis discovered by probing the metal, pH, and solvent isotope effects.

Many kinases have been reported to bind to a second metal ion for catalytic activity in addition to the one required to form the nucleotide−metal complex. Mg^{2+} is considered the physiological metal of kinases because of its high concentration in the cell compared with those of other divalent metal ions, although catalytic activity is detected also with Mn^{2+}, Co^{2+}, and, Cd^{2+} (*9*, *10*). Herein we report that (1) cdk5/p25-catalyzed H1P phosphorylation requires the binding of a second Mg^{2+} for its catalytic activity, (2) the binding of the second Mg^{2+} induces a conformational change that does not limit the access of either substrate, although it favors ATP binding, and (3) in the presence of the second Mg^{2+} the phosphoryl transfer step is the rate-limiting step and associated with a single proton transfer, which is facilitated by a general acid−base catalyst.

MATERIALS AND METHODS

Materials. Adenosine 5′-triphosphate (ATP), phosphoenolpyruvate, magnesium chloride, NADH, 2-(*N*-morpholino)propanesulfonic acid (MOPS), trichloroacetic acid (TCA), bovine serum albumin, pyruvate kinase type II from rabbit muscle, and lactate dehydrogenase type II from bovine heart were purchased from Sigma (St. Louis, MO). Dithiothreitol (DTT) was from Fluka (St. Louis, MO). Histone H1-derived peptide PKTPKKAKKL (H1P) was purchased from Anaspec (San Jose, CA). H1P analogue $H1P^{Ala}$ (PKAPKKAKKL) was purchased from American peptides (Sunnyvale, CA). [γ-^{33}P]ATP was from PerkinElmer (Boston, MA). cdk5/p25 was generously provided by K. Kosik (University of California, Santa Barbara, CA).

Kinetic Analysis of H1P Phosphorylation by cdk5/p25. The kinase assay was conducted in buffer containing 20 mM MOPS (pH 7.5), 1 mM DTT, 0.5 mg/mL BSA, $MgCl_2$, H1P (PKTPKKAKKL), ATP, and [γ-^{33}P]ATP. The reactions were conducted in triplicate and initiated by the addition of 7.8 nM cdk5/p25, and the mixtures were incubated at room temperature for 30 min. The reaction was stopped by the addition of 10 mM EDTA, and the mixture was transferred to a multiscreen PH filtration plate (Millipore, Billerica, MA) and washed six times

*To whom correspondence should be addressed: Laboratory for Drug Discovery in Neurodegeneration, Harvard NeuroDiscovery Center, 65 Landsdowne St., Fourth Floor, Cambridge, MA 02139. Phone: (617) 768-8658. Fax: (617) 768-8606. E-mail: mliu@rics.bwh.harvard.edu.

[1]Abbreviations: AD, Alzheimer's disease; cdk5/p25, cyclin-dependent kinase 5; H1P, histone H1-derived peptide PKTPKKAKKL; $H1P^{Ala}$, PKAPKKAKKL; $H1P^{DaP}$, PKDapPKKAKKL.

Published on Web 05/21/2010

with 75 mM H_3PO_4. The filters were removed, and the samples were counted with a scintillation counter. The background reaction was conducted in the absence of H1P. In all cases, reaction progress curves for production of the phosphoprotein were linear over at least 45 min and allowed calculation of initial velocities.

Buffer Salts for pH Dependencies. In all of these kinetic studies, reaction solutions contained 20 mM buffer salt, 50 mM NaCl, 2.5 mM $MgCl_2$, 1 mM DTT, and 0.5 mg/mL BSA. The following buffer salts were used: MES at pH 5.5−6.5, PIPES at pH 6.5−7.0, HEPES at pH 7.0−8.0, HEPBS at pH 8.5−9.0, and CHES at pH 9.5−10.0.

Data Analysis. Data were analyzed by a nonlinear least-squares method, using either Sigma-Plot or Grafit. Standard kinetic mechanisms for two-substrate reactions and their rate equations are shown below:

Ping-pong:

$$v = \frac{k_{cat}[E][A][B]}{K_A[B] + K_B[A] + [A][B]} \quad (1)$$

where K_A and K_B are Michaelis constants.

Rapid equilibrium ordered:

$$v = \frac{k_{cat}[E][A][B]}{K_A K_B + K_B[A] + [A][B]} \quad (2)$$

where K_A and K_B are substrate dissociation constants for the E·A and E·B complexes, respectively.

Rapid equilibrium random/steady-state ordered:

$$v = \frac{k_{cat}[E][A][B]}{\alpha K_A K_B + \alpha K_A[B] + \alpha K_B[A] + [A][B]} \quad (3)$$

Replot equations for a random mechanism:

$$(k_{cat})_A = k_{cat}\left(\frac{[B]}{\alpha K_B + [B]}\right) \quad (4)$$

$$(k_{cat}/K_m)_A = \frac{k_{cat}}{\alpha K_A}\left(\frac{[B]}{K_B + [B]}\right) \quad (5)$$

For rapid equilibrium systems, K_A, K_B, αK_A, and αK_B are substrate dissociation constants for E·A, E·B, and E·A·B complexes. For steady-state systems, K_A is the substrate dissociation constant for the E·A complex and αK_A and αK_B are Michaelis constants. See ref *11* for definitions of mechanisms, substrate dissociation constants, and α.

RESULTS

Initial Velocity Studies. The effect of free Mg^{2+} on cdk5/p25-catalyzed H1P phosphorylation was studied by the use of initial velocity studies as discussed by Cook (*12*, *13*). Experiments were performed in which the initial velocities were measured as a function of H1P concentration, at several fixed concentrations of MgATP (331, 166, 83, 42, and 21 μM) and at a single fixed concentration of free Mg^{2+} at 0.2 mM (Figure 1A). This experiment was repeated at four concentrations of free Mg^{2+}, 0.6, 1.3, 2.5, and 5 mM. Magnesium ions in excess of that needed to bind ATP were assumed to be free Mg^{2+}, and the dissociation constant of MgATP (14.3 μM) (*14*) was used to calculate the concentrations of MgATP and free Mg^{2+}. Extra care and calculation were used to keep the concentration of free Mg^{2+} as a constant for the entire MgATP concentration range. To make it easier, in the rest of the text ATP is used to represent the real substrate MgATP. Each data set was subjected to global analysis by nonlinear least-squares fits to the equations that reflect ping-pong, rapid equilibrium ordered, and random/steady-state ordered mechanisms (eqs 1−3). Statistically, the data fit the equation reflecting the rapid equilibrium random/steady-state ordered mechanism the best, and the parameters analyzed for 0.2 and 2.5 mM Mg^{2+} are summarized in Table 1. To examine the data carefully and judge among the mechanisms, we also used the method of replots as described previously (*8*). The starting point in this data analysis was to calculate apparent values of $(k_{cat})_X$ and $(k_{cat}/K_m)_X$ (X is H1P or ATP) by nonlinear least-squares fits of each individual plot of v_o versus [X] in the primary data sets to the simple Michaelis−Menten equation. The next step in this analysis was to construct the replots of the dependencies of apparent values of $(k_{cat})_A$ and $(k_{cat}/K_m)_A$ on [B] and the dependencies of apparent values of $(k_{cat})_B$ and $(k_{cat}/K_m)_B$ on [A] and examine their shape. Replots will show a specific, mechanism-based pattern. For example, for the random mechanism of eq 3, apparent values of $(k_{cat})_A$ and $(k_{cat}/K_m)_A$ will be

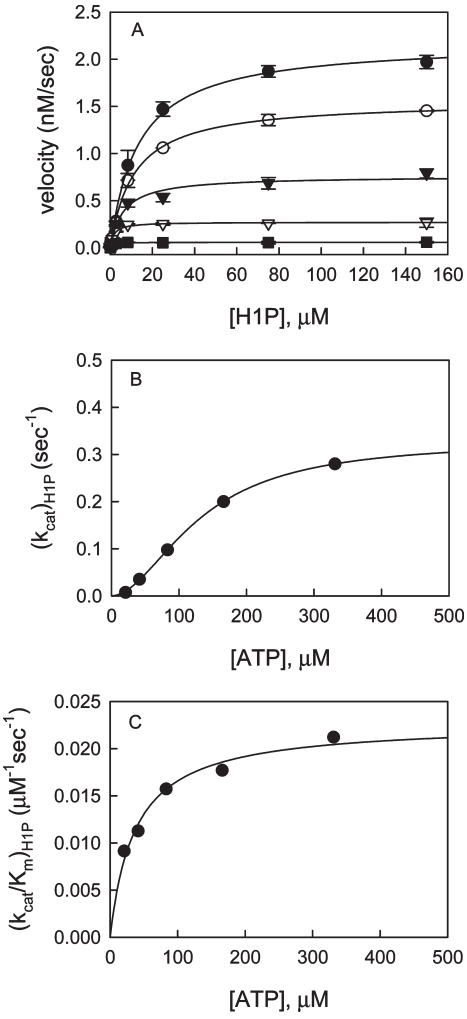

FIGURE 1: Steady-state kinetic experiment for cdk5/p25-catalyzed H1P phosphorylation at a free Mg^{2+} concentration of 0.2 mM. (A) Dependence of initial velocity on H1P concentration at ATP (or MgATP as in the text) concentrations of 331 (●), 166 (○), 83 (▼), 41.5 (▽), and 21 μM (■). Each data point is the average of duplicate measurements. The data were globally fit to the equation reflecting the rapid equilibrium random/steady-state mechanism. (B and C) ATP concentration dependencies of $(k_{cat})_{H1P}$ and $(k_{cat}/K_m)_{H1P}$. Apparent values of $(k_{cat})_{H1P}$ and $(k_{cat}/K_m)_{H1P}$ were calculated by fitting the individual plot of v_0 vs [H1P] of panel A to the simple Michaelis−Menten equation.

Table 1: Initial Velocity Analysis for cdk5/p25-Catalyzed H1P Phosphorylation at Low and High Free Mg^{2+} Concentrations[a]

	0.2 mM Mg^{2+}	2.5 mM Mg^{2+}
k_{cat} (s^{-1})	0.77 ± 0.04	3.6 ± 0.2
K_{H1P} (μM)	12 ± 0.7	7 ± 0.5
K_{ATP} (μM)	60 ± 20	6.1 ± 1.5
α	16 ± 2	12 ± 1.7

[a]The parameter estimates were calculated by globally fitting the data to the equation reflecting the rapid equilibrium random/steady-state order mechanism. Each parameter estimate is the average of two independent experiments. The error limit is the deviation from the mean.

hyperbolically dependent on [B] according to the equations given in eqs 4 and 5. Likewise, apparent values of $(k_{cat})_B$ and $(k_{cat}/K_m)_B$ will be hyperbolically dependent on [A].

Replots of apparent values of $(k_{cat})_{H1P}$ and $(k_{cat}/K_m)_{H1P}$ versus [ATP] and apparent values of $(k_{cat})_{ATP}$ and $(k_{cat}/K_m)_{ATP}$ versus [H1P] through the whole range of free Mg^{2+} concentrations all revealed hyperbolic dependencies on substrate concentration, suggesting that the reaction follows either a random or a steady-state ordered mechanism. Examples of these replots at 0.2 mM Mg^{2+} are shown in panels B and C of Figure 1. A sigmoid kinetic behavior was observed in Figure 1B, and data were fitted to an equation reflecting sigmoidicity $\{v = v_c/[1 + (K_S/[S])^n]\}$, yielding a Hill coefficient of 1.8 ± 0.1. To distinguish between the two mechanisms, we conducted substrate analogue and product inhibition studies (see below).

Next we examined the effects of Mg^{2+} on the steady-state kinetic parameters, and the results are shown in Figure 2. A level of zero free Mg^{2+} cannot be achieved in the presence of MgATP; therefore, the effect of zero free Mg^{2+} can only be extrapolated from higher Mg^{2+} concentrations. Increasing the free Mg^{2+} concentration resulted in an increase in k_{cat}, with the maximal k_{cat} being achieved at 5 mM Mg^{2+} (Figure 2A). Increasing the free Mg^{2+} concentration also resulted in an increase in k_{cat}/K_{H1P} (Figure 2B), which is mainly due to the increase in k_{cat} at high Mg^{2+} concentrations. The values of K_{H1P} remain almost the same through the entire Mg^{2+} concentration range, 12 ± 0.7 μM at 0.2 mM free Mg^{2+}, 11 ± 0.8 μM at 1.3 mM free Mg^{2+}, and 7 ± 0.5 μM at 2.5 mM free Mg^{2+}. However, the values of K_{MgATP} decrease with an increasing free Mg^{2+} concentration, 60 ± 20 μM at 0.2 mM free Mg^{2+} and 6.1 ± 1.5 μM at 2.5 mM free Mg^{2+}. The much lower sensitivity at low Mg^{2+} concentrations contributed to the large error in K_{ATP}. The increases in both k_{cat} and ATP binding affinity lead to an increase in k_{cat}/K_{ATP} (Figure 2C). The data in panels A and B of Figure 2 were fitted to an expression of enzyme activation that requires binding of one activator to achieve full activity $[v = v_c/(1 + K_A/[A])]$, yielding dissociation constants for Mg^{2+} of 0.6 ± 0.07 and 0.6 ± 0.2 mM under the conditions of k_{cat} and k_{cat}/K_{H1P}. A sigmoid kinetic behavior was observed under the condition of k_{cat}/K_{ATP} (Figure 2C), and data were fitted to an equation reflecting sigmoidicity $\{v = v_c/[1 + (K_A/[A])^n]\}$, yielding dissociation constant for Mg^{2+} of 1.7 ± 0.1 mM and a Hill coefficient of 2.1 ± 0.3.

To ensure that the additional magnesium requirement is not a result of a nonspecific ionic effect, we measured cdk5/p25 activity at different NaCl concentrations. The activity of cdk5 remained the same at NaCl concentrations of < 80 mM but decreased at high concentrations of NaCl (data not shown).

Inhibition Studies with Substrate Analogues and Product ADP. To determine the kinetic mechanism of cdk5/p25-catalyzed H1P phosphorylation at low Mg^{2+} concentrations, inhibition

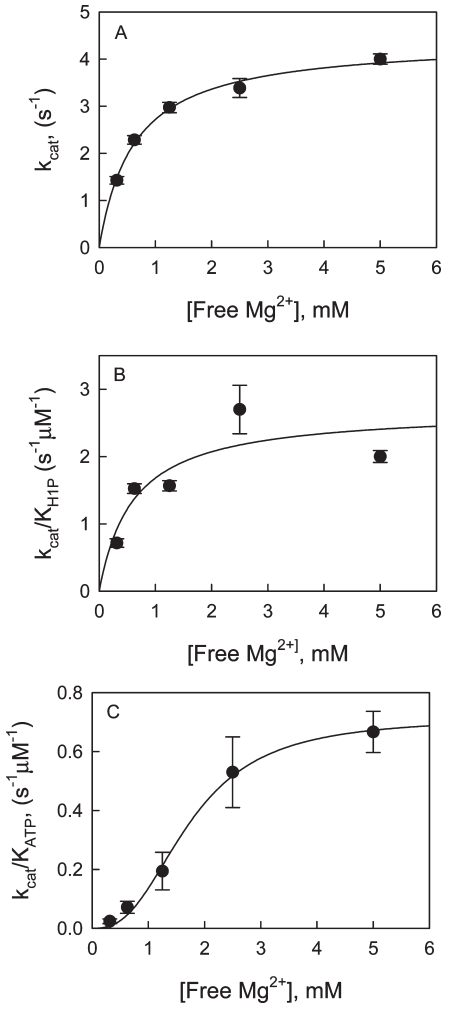

FIGURE 2: Effect of free Mg^{2+} on steady-state parameters. Dependencies of (A) k_{cat}, (B) k_{cat}/K_{H1P}, and (C) k_{cat}/K_{ATP} on free Mg^{2+} concentration.

studies were conducted with nucleotide analogue AMP, product ADP, and peptide substrate analogue $H1P^{Ala}$ (PKAPKKAKKL) at 0.2 mM $MgCl_2$. We first determined at several concentrations of inhibitor (i) the dependence of v_0 on [H1P] at a single ATP concentration and (ii) the dependence of v_0 on [ATP] at a single H1P concentration. Examples of the ATP concentration dependence of the initial velocity for AMP and $H1P^{Ala}$ inhibition are shown in panels A and D of Figure 3. Next we analyzed (i) the dependence of v_0 on [H1P] at each [I] and (ii) the dependence of v_0 on [ATP] at each [I] by a nonlinear least-squares fit to the simple Michaelis−Menten equation to calculate apparent values of $(k_{cat})_X$ and $(k_{cat}/K_m)_X$ (X is ATP or H1P). Finally, in this analysis, we constructed the replots of apparent values of $(k_{cat})_X$ versus [I] and apparent values of $(k_{cat}/K_m)_X$ versus [I]. Examples of these replots for AMP as an inhibitor are shown in panels B and C of Figure 3, and examples for $H1P^{Ala}$ are shown in panels E and F of Figure 3. We found that when ATP was the variable substrate (i) for AMP or ADP inhibition, $(k_{cat})_{ATP}$ is independent of AMP or ADP and $(k_{cat}/K_m)_{ATP}$ titrates with AMP or ADP according to the simple inhibition expression of the general form $v_{inhib} = v_{control}/(1 + [I]/K_{i,app})$ and (ii) for $H1P^A$ inhibition, $(k_{cat})_{ATP}$ is independent of $H1P^{Ala}$ and $(k_{cat}/K_m)_{ATP}$ titrates with $H1P^{Ala}$. We found that when H1P was the variable substrate (i) for AMP or ADP inhibition, both $(k_{cat})_{H1P}$ and $(k_{cat}/K_m)_{H1P}$ titrate with AMP or ADP and (ii) for $H1P^{Ala}$ inhibition, $(k_{cat})_{H1P}$ is independent of $H1P^{Ala}$ and

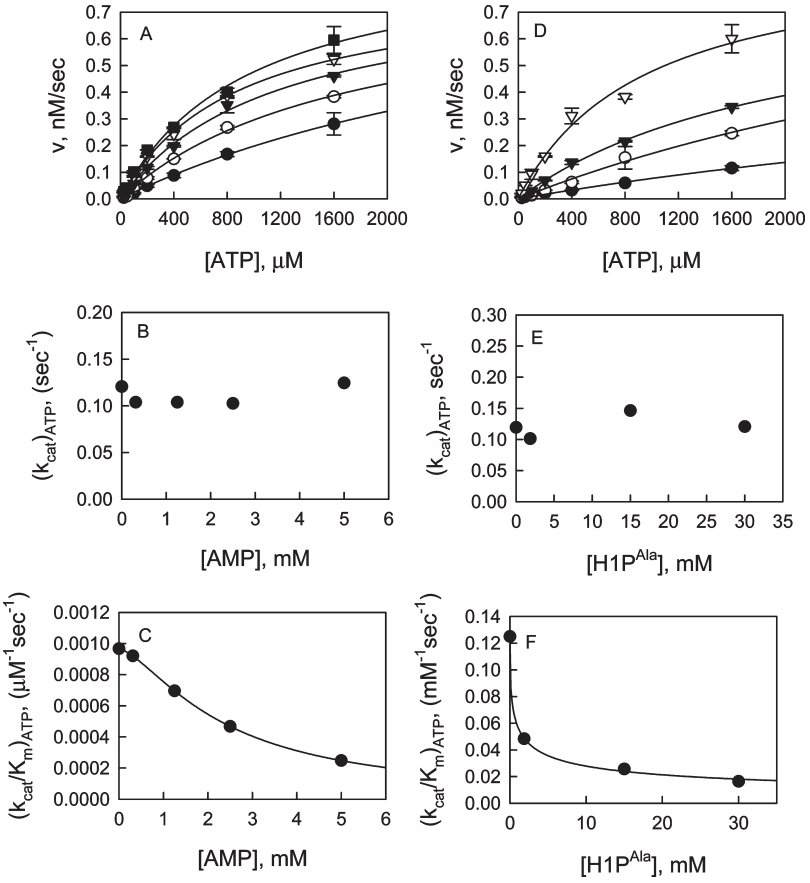

FIGURE 3: Inhibition of the cdk5/p25-catalyzed H1P phosphorylation by substrate analogues H1P^{Ala} and AMP at 0.2 mM Mg^{2+}. Inhibition by H1P^{Ala}: (A) dependence of $K_{i,app}$ on H1P and (B) dependence of $K_{i,app}$ on ATP. Inhibition by AMP: (C) dependence of $K_{i,app}$ on ATP and (D) dependence of $K_{i,app}$ on H1P.

Scheme 1: Rapid Equilibrium Random Mechanism of cdk5/p25-Catalyzed Phosphorylation[a]

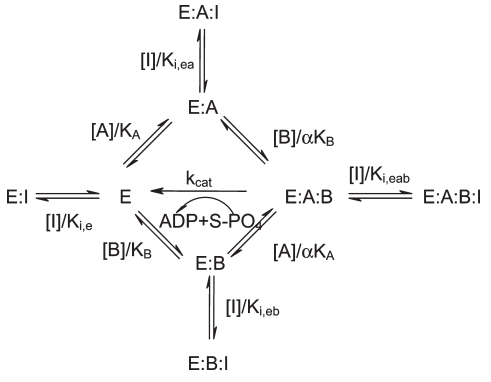

[a]A represents ATP, and B represents H1P.

$(k_{cat}/K_m)_{H1P}$ titrates with H1P^{Ala}. This suggests that H1P^{Ala} is competitive with both ATP and H1P; AMP or ADP is competitive with ATP and noncompetitive with H1P.

These patterns rule out a steady-state ordered mechanism but are different from the ones well-known for a rapid equilibrium random mechanism in which it has been assumed that the competitive inhibitors act as dead-end inhibitors and bind to the same enzyme form as the substrates (*15*). The patterns seen in this study clearly suggest that the inhibitors interact with the enzyme in a different mode. To examine these results and estimate the values of dissociation constants, we used the method previously described in detail (*8*), where the general mechanism of Scheme 1, in which inhibitor can bind to all four forms of enzyme, was used to derive the rate equation (eq 6) under rapid equilibrium conditions.

$$v = \frac{\dfrac{k_{cat}[E][A]}{1+\dfrac{\alpha K_B}{[B]}+\dfrac{\alpha K_B}{[B]}\dfrac{[I]}{K_{i,ea}}+\dfrac{[I]}{K_{i,eab}}}}{K_A\left\{\dfrac{\alpha+\dfrac{\alpha K_B}{[B]}+\dfrac{\alpha K_B}{[B]}\dfrac{[I]}{K_{i,e}}+\dfrac{[I]}{K_{i,eab}}}{1+\dfrac{\alpha K_B}{[B]}+\dfrac{\alpha K_B}{[B]}\dfrac{[I]}{K_{i,ea}}+\dfrac{[B]}{K_{i,eab}}}\right\}+[A]} \quad (6)$$

By inspecting eqs 7−10 which describe the dependencies of apparent values $(k_{cat})_X$ and $(k_{kcat}/K_m)_X$ (X is ATP or PLK-peptide) on inhibitor, we can immediately see how inhibitors interact with the enzyme.

$$(k_{cat})_{ATP} = \frac{k_{cat}[E]}{1+\dfrac{\alpha K_B}{[B]}+\dfrac{\alpha K_B}{[B]}\dfrac{[I]}{K_{i,ea}}+\dfrac{[I]}{K_{i,eab}}} \quad (7)$$

$$(k_{cat}/K_m)_{ATP} = \frac{k_{cat}[E]/\alpha K_A}{1+\dfrac{K_B}{[B]}+\dfrac{K_B}{[B]}\dfrac{[I]}{K_{i,e}}+\dfrac{[I]}{\alpha K_{i,eab}}} \quad (8)$$

In the case of H1P^{Ala} inhibition where ATP is the variable substrate, $(k_{cat})_{ATP}$ is independent of H1P^{Ala}, which suggests that both $K_{i,ea}$ and $K_{i,eab}$ are very large and H1P^{Ala} cannot bind to either the E·A or E·A·B complex. On the other hand, $(k_{cat}/K_m)_{ATP}$ titrates with H1P^{Ala}, suggesting that H1P^{Ala} can bind to

Table 2: Inhibition of Cdk5/p25 by Substrate Analogues at 0.2 mM Mg^{2+}

	substrate			inhibition constant (mM)	
inhibitor	fixed	variable	mechanism	$K_{i,e}$	$K_{i,es}$
AMP	ATP	H1P	noncompetitive	2.7 ± 0.3	1.4 ± 0.5
	H1P	ATP	competitive	2.5 ± 0.7	
ADP	ATP	H1P	noncompetitive	0.6 ± 0.1	0.3 ± 0.1
	H1P	ATP	competitive	0.3 ± 0.1	
$H1P^{Ala}$	ATP	H1P	competitive	0.2 ± 0.1	
	H1P	ATP	competitive	0.6 ± 0.3	

E, the E·B complex, or both. It is clear that at this point we cannot calculate independent estimates of $K_{i,e}$ and $K_{i,eb}$.

We can, however, obtain this information by inspecting eqs 9 and 10. In the case where PLK-peptide is the variable substrate, $(k_{cat})_{PLK}$ is independent of $H1P^{Ala}$ which suggests that both $K_{i,eb}$ and $K_{i,eab}$ are very large and $H1P^{Ala}$ cannot bind to either the E·B complex or the E·A·B complex; $(k_{cat}/K_m)_{PLK}$ titrates with $H1P^{Ala}$, suggesting that $H1P^{Ala}$ can bind to E or the E·A complex.

$$(k_{cat})_{PLK} = \frac{k_{cat}[E]}{1+\frac{\alpha K_A}{[A]}+\frac{\alpha K_A}{[A]}\frac{[I]}{K_{i,eb}}+\frac{[I]}{K_{i,eab}}} \quad (9)$$

$$(k_{cat}/K_m)_{PLK} = \frac{k_{cat}[E]/\alpha K_B}{1+\frac{K_A}{[A]}+\frac{K_A}{[A]}\frac{[I]}{K_{i,e}}+\frac{[I]}{\alpha K_{i,ea}}} \quad (10)$$

Using this method, we can identify the enzyme forms that inhibitors bind and estimate the dissociation constants as follows. (i) $H1P^{Ala}$ binds only to free enzyme, and $K_{i,e}$ was estimated directly from eq 8 or 10 with our previous knowledge of k_{cat}, K_A, K_B, and α. (ii) AMP behaves as a dead-end inhibitor and binds to both E and the E·B complex. $K_{i,eb}$ was estimated directly from eq 9, $K_{i,e}$ directly from eq 10, and $K_{i,e}$ also from use of $K_{i,eb}$ and eq 8. The mechanism of inhibition and dissociation constants for $H1P^{Ala}$, AMP, and ADP at low Mg^{2+} concentrations are summarized in Table 2.

pH Dependence of Steady-State Kinetic Parameters of H1P Phosphorylation. We determined the pH stability of cdk5/p25 by incubating the enzyme at the desired pH and assaying aliquots at pH 7. Enzyme is stable from pH 6 to 9. A small activity loss occurs at pH 5.5 and 10.0. The phosphorylation of H1P was monitored over a pH range of 5.5−10.0 under conditions of variable H1P (0−480 μM) and fixed ATP (800 μM) at a high Mg^{2+} concentration (5 mM). Plots of v_0 versus H1P concentration were used to determine k_{cat} and k_{cat}/K_{H1P}. The pH profile of k_{cat} showed a bell-shaped curve (Figure 4) and was fitted to eq 11, yielding two apparent pK_a values of 6.1 and 10.0. The involvement of an alkaline residue in the catalysis is questionable because of the activity loss at the higher pH due to protein denaturation. Also, an alkaline group with a pK_a of 8.3 was revealed in the ATPase reaction (see below). It is possible that the activity loss at higher pH could simply be due to protein denaturation rather than the titration of an alkaline residue. k_{cat}/K_{H1P} exhibited a pH dependence similar to that of k_{cat} due to the pH insensitivity of K_{H1P} (data not shown).

$$y = \frac{C}{1+10^{-pH}/10^{-pK_{a1}}+10^{-pK_{a2}}/10^{-pH}} \quad (11)$$

As mentioned in the previous study, cdk5/p25 possesses an ATPase activity with a k_{cat} value 15-fold lower than that for the kinase activity. Since the transfer to water is slow, the phosphoryl transfer rate is almost certain to be rate-determining. A pH study was conducted for the cdk5/p25-catalyzed ATP hydrolysis. The K_m values for ATP were found to be 20, 11, 8, and 10 μM at pH 6, 7, 8, and 9, respectively. The pH profile of k_{cat} for ATP hydrolysis showed a bell-shaped curve and was fit to eq 11, yielding two apparent pK_a values of 6.3 and 8.3 as shown in Figure 5A. The bell-shaped curve was also found in the pH profile of k_{cat}/K_{ATP} without perturbation of two pK_a values when the data were fit to eq 11 as shown in Figure 5B. Buffer crossover experiments revealed no dependence on the buffer salt. Comparison of the pH profiles of k_{cat} of the kinase and ATPase reactions revealed similar pK_a values on the acid side, while the alkaline pK_a values are quite different. It is possible that the group giving rise to the alkaline pK_a in the ATPase reaction is no longer involved in catalysis.

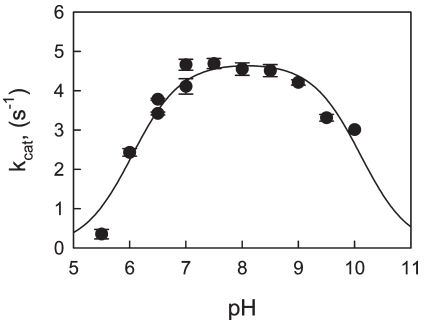

FIGURE 4: pH dependence of k_{cat} for the cdk5/p25-catalyzed H1P phosphorylation. The experiments were conducted under conditions of variable H1P (0−480 μM) and fixed ATP (800 μM) at 5 mM Mg^{2+}. The data were fit to eq 11.

Proton Inventory Study. The proton inventory study was conducted for k_{cat} (initial velocity measured at saturating concentrations of both ATP and H1P) at low (0.2 mM) and high (5 mM) Mg^{2+} concentrations in the mixture of H_2O and D_2O at pH 7.4 and the pD equivalent. The dependence of the ratio of k_{cat} (k_n/k_0) in the presence and absence of varying atom fractions of D_2O (n) on n at high and low Mg^{2+} concentrations is presented in Figure 6. At high Mg^{2+} concentrations, k_n/k_0 decreases linearly with n. The solvent deuterium isotope effect on k_{cat} can be expressed by the linear form of the Gross−Butler equation (eq 12) with only one exchangeable hydrogen site:

$$k_n/k_0 = (1-n+n\phi^T)/(1-n+n\phi^R) \quad (12)$$

where ϕ^R and ϕ^T are fractionation factors for the exchangeable hydrogen in the reactant and transition states, respectively. The fitting of data to the equation gives the following estimates: $\phi^R = 1$ and $\phi^T = 0.47$. Given this, we can assign the estimate to SKIE for k_{cat} ($^D k_{cat} = \phi^R/\phi^T = 2.0 \pm 0.1$, determined from three independent experiments). To make certain that changes in side chain pK_a values in light and heavy water are not causing a dramatic difference in SKIE, the proton inventory study for k_{cat} was repeated at low (0.2 mM) and high (5 mM) Mg^{2+} concentrations in the mixture of H_2O and D_2O at pH 8.0 and the pD equivalent. No dramatic differences in SKIE were observed, and SKIE values of 1.8 ± 0.1 and 1.0 ± 0.1 were determined from three independent experiments at high and low Mg^{2+} concentrations. At low Mg^{2+} concentrations, a linear proton inventory and SKIE value of 1.1 ± 0.1 were observed for k_{cat} (Figure 6). The proton inventory study was also conducted at high and low Mg^{2+} concentrations on k_{cat}/K_{H1P} (initial velocity measured at a saturating concentration of

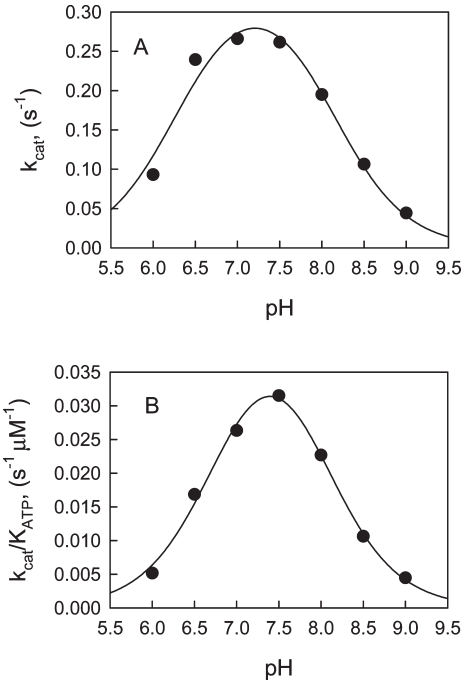

FIGURE 5: pH profiles of the ATPase reaction of cdk5/p25. (A) pH dependence of k_{cat} and (B) pH dependence of k_{cat}/K_{ATP}. The experiments were conducted under conditions of variable ATP at 5 mM Mg^{2+}. The data were fit to eq 11.

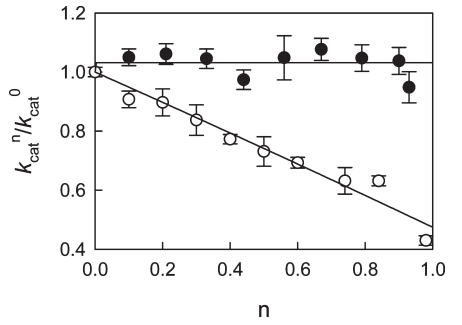

FIGURE 6: Proton inventory of k_{cat} for the cdk5/p25-catalyzed H1P phosphorylation at 5 (○) and 0.2 mM Mg^{2+} (●). k_{cat}^{n}/k_{cat}^{0} is the ratio of k_{cat} in the presence and absence of varying atom fractions of deuterium (n). Initial velocities were determined at saturating concentrations of both ATP and H1P.

ATP and a concentration of H1P 10-fold less than K_{H1P}) and k_{cat}/K_{ATP} (initial velocity measured at a saturating concentration of H1P and a concentration of ATP 10-fold less than K_{ATP}) in three independent experiments. At both high and low Mg^{2+} concentrations, linear proton inventory and SKIE values close to 1 were found for these parameters and are summarized in Table 3.

Influence of D_2O on Inhibitor Binding. The dissociation constant for the ATP competitive inhibitor AMP was measured in pure H_2O and 85% D_2O in 10 μM ATP and at a saturating H1P concentration. The dependence of v_0 on [I] was analyzed by a nonlinear least-squares fit to the expression $v_{inhi} = v_{control}/(1 + [I]/K_{i,app})$ to determine $K_{i,app}$.

DISCUSSION

Many kinases have been reported to bind to a second metal ion in addition to the one required to form the nucleotide−metal complex, though the role of the second metal varies in each case. For example, a second metal ion activates Csk and Src by increasing the k_{cat} without affecting the K_{ATP} (*16*). However, it activates IRK and v-Fps by decreasing the K_{ATP} without affecting the k_{cat} (*17*, *18*). More interestingly, the second Mg^{2+} binding in the active site of cAMP-dependent protein kinase (PKA) inhibits the kinase activity by decreasing its k_{cat} (*19*). In this study, we report the effect of the second Mg^{2+} on the cdk5/p25-catalyzed H1P phosphorylation.

Table 3: SKIE Parameters for the cdk5/p25-Catalyzed H1P Phosphorylation at Low and High Free Mg^{2+} Concentrations[a]

	0.2 mM Mg^{2+}	2.5 mM Mg^{2+}
$^{D}(k_{cat})$	1.1 ± 0.1	2.0 ± 0.1
$^{D}(k_{cat}/K_A)$	1.0 ± 0.1	1.0 ± 0.1
$^{D}(k_{cat}/K_B)$	1.0 ± 0.1	1.0 ± 0.1

[a]The dependence of the ratio of each kinetic parameter on varying atom fractions of D_2O (n) was fit to the Gross−Bulter equation: $k_n/k_0 = (1 - n + n\phi^T)/(1 - n + n\phi^R)$. SKIE was estimated as the ϕ^R/ϕ^T ratio. Each parameter estimate is the average of three independent experiments. The error limit is the deviation from the mean.

Kinetic Mechanism. The initial velocity study of the cdk5/p25-catalyzed H1P phosphorylation at different concentrations of Mg^{2+} revealed that a second Mg^{2+} is required to bind to cdk5/p25 for its catalytic activity. It activates cdk5/p25 by demonstrating an increase in k_{cat}. The binding of the second Mg^{2+} facilitates ATP binding by demonstrating a dramatic decrease in K_{ATP}. Likewise, the binding of ATP also favors the binding of the second Mg^{2+}; the saturation of ATP in the active site decreases the dissociation constant of the second Mg^{2+} by 3-fold. More surprisingly, sigmoid kinetic behavior was observed for the binding of ATP at low Mg^{2+} concentrations and the binding of Mg^{2+} at low ATP concentrations, as demonstrated by a Hill coefficient of ~2 in each case. At either low Mg^{2+} or low ATP concentrations, the two subunits of the cdk5/p25 dimer interact cooperatively and permit a much more sensitive response to the ligand concentration (either ATP or Mg^{2+}). On the other hand, the presence of the second Mg^{2+} makes this type of cooperative interaction unnecessary by inducing a conformational change that favors ATP binding without limiting the access of either substrate. A rapid equilibrium random mechanism in the absence of the second Mg^{2+} was revealed by substrate analogue and product inhibition studies, which is consistent with a random mechanism in the presence of the second Mg^{2+} as reported in a previous study (*8*).

The discrete mechanism of the second Mg^{2+} coordinated in its interaction with cdk5/p25 is kinetically complex. It might bind to a site other than the active site of the enzyme and induce a conformational change. This hypothesis is supported by the crystal structure of cdk2, which is a member of the cyclin-dependent kinase family and is 60% identical with cdk5 in terms of sequence. In the cocrystal structure of cdk2-cyclinA3 with both a peptide substrate and an ATP analogue, there is only one bound Mg^{2+} chelating the α- and γ-phosphates in the active site (*20*). It is also possible that the second metal was not observed in the crystalline state due to the experimental conditions (the crystal was grown in the presence of 5 mM Mg^{2+}), and it is actually coordinated within the active site of the enzyme and participates in catalysis directly. This hypothesis is supported by the mutual effects of free Mg^{2+} and ATP observed on the binding of the other: the K_{ATP} was lowered by 10-fold at saturating Mg^{2+} concentrations, and likewise, the K_d of free Mg^{2+} was decreased significantly at saturating ATP concentrations. Many kinases

require a second metal ion for the catalytic activity, such as phosphoenolpyruvate carboxykinase (PEPCK), protein tyrosine kinase, and LRRK2 (*21*−*23*). Evidence from these kinases also supports the second hypothesis. For example, the crystallographic structure of PEPCK revealed the coexistence of Mg^{2+} and Mn^{2+} in the active site at two distinct locations (*22*). The two metal ions make contacts with ATP and different amino acid residues, with Mg^{2+} chelating both the β- and γ-phosphate of ATP. We propose that the second Mg^{2+} directly binds to the active site of cdk5/p25 and makes contact with the β- or γ-phosphate of ATP through either direct or water-mediated interactions.

The fact that Mg^{2+} modulates the activity of cdk5/p25 may have physiological consequences worth noting. The activity of cdk5/p25 could be modulated in vivo by changes in the free cytoplasmic Mg^{2+} concentration.

Proton Transfer. On the basis of the chemical principle of phosphoryl transfer, the hydroxyl proton must be removed to form products. Therefore, the study of phosphoryl transfer catalyzed by kinases is inevitably linked to the study of its proton transfer mechanism. To further our understanding of the role of the second Mg^{2+} in H1P phosphorylation, we conducted a proton inventory study at both high and low Mg^{2+} concentrations. The use of the shape of the proton inventory and the size of the solvent isotope effect to determine the number of hydrogenic sites and diagnose the mechanism have been well discussed by Schowen and Venkatasubban (*25*, *26*).

(*i*) *Proton Transfer and Rate-Determining Step at High Mg^{2+} Concentrations*. A normal SKIE (2.0) was observed on k_{cat} at high Mg^{2+} concentrations. To interpret the effect of the isotope on cdk5/p25-catalyzed H1P phosphorylation, it is important to know whether the larger intrinsic viscosity of D_2O or an equilibrium isotope effect on a catalytic residue or on buffer pK_a provided the source for the observed SKIE. First, the observed SKIE is much larger than the predicted influence of D_2O due to viscosity. Since D_2O is 20% more viscous than H_2O, the effects of increased viscosity would account for only 5% rather than the observed 50% change in turnover rate. Second, the lack of a SKIE on kinetic parameters at low Mg^{2+} concentrations (see below) ruled out the possibility that the observed SKIE is due to an equilibrium isotope effect. With these as foundations, proton inventory can be interpreted. The linear proton inventory with a normal SKIE (2.0) observed with k_{cat} at a high Mg^{2+} concentration suggests that (i) a single protonic interaction in the catalytic transition state is responsible for the solvent isotope effect (that is, one-proton catalysis) and binding at this protonic site is looser in the transition state than in the reactant state and (ii) phosphoryl transfer is the rate-limiting step of the process governed by k_{cat}. In an independent study that aimed to measure the pre-steady-state kinetics using a rapid quench flow technique, the phosphorylation of H1P exhibited no burst kinetics for k_{cat} which is consistent with a slow phosphoryl transfer and a rapid product release mechanism (data not shown).

Since the enzyme follows a rapid equilibrium random mechanism at high Mg^{2+} concentrations, it is reasonable to assume that the substrate is in rapid exchange with the enzyme. As a result, a SKIE is anticipated in the parameter k_{cat}/K_{H1P} or k_{cat}/K_{ATP}. Surprisingly, no SKIE was observed in either. The lack of a SKIE on k_{cat}/K_{H1P} or k_{cat}/K_{ATP} may suggest that during the process governed by k_{cat}/K_m, the enzyme−substrate complex (E·A or E·S) undergoes a slow deuterium-insensitive step preceding the phosphoryl transfer step, but the inhibition data suggest another solution. The dissociation constant for dissociation of AMP from the E·H1P·AMP complex was found to be lower in 85% D_2O than in water by approximately 1.5-fold (data not shown). The solvent isotope effect on the dissociation constant originates from solvent reorganization that accompanies substrate or inhibitor binding and generally ranges from 1.2 to 1.8 (*27*). On the basis of a predicted SKIE of 1.6 for k_{cat} at 85% D_2O, the equilibrium isotope effect on substrate binding offsets the SKIE so that no SKIE is observed for k_{cat}/K_{ATP} or k_{cat}/K_{H1P}. Scheme 2 depicts the random mechanism for cdk5/p25-catalyzed H1P phosphorylation at high Mg^{2+} concentrations, where the E·S or E·A binary substrate complex binds to the second substrate to form the E·ATP·S active central complex controlled by the association rate constant k_2 and dissociation rate constant k_{-2}. The catalytic step, k_3, describes the unimolecular rate constant for the chemical transfer as well as any conformational change associated with this step. Finally, the release of product and the conformational change associated with it are combined in k_4. Rate equations for k_{cat} and k_{cat}/K_m of Scheme 2 were derived by using Cleland's methods of net rate constants (*28*):

Scheme 2

$$\underset{\text{(or E:S)}}{\text{E:A}} \underset{k_{-2}}{\overset{k_2[\text{B}]}{\rightleftharpoons}} \text{E:A:B} \xrightarrow{k_3} \text{E:P:Q} \xrightarrow{k_4} \text{E + P + Q}$$

$$k_{cat} = k_3k_4/(k_3 + k_4) \quad (13)$$

$$k_{cat}/K_m = k_2k_3/(k_{-2} + k_3) \quad (14)$$

Due to the relatively rapid process of product release ($k_4 > k_3$), k_{cat} becomes approximately equal to k_3. On the basis of the assumption that substrate is in rapid exchange with the enzyme (i.e., $k_{-2} > k_3$), k_{cat}/K_m could be simplified into the expression as in eq 15.

$$k_{cat}/K_m = k_2k_3/k_{-2} \quad (15)$$

We commonly refer to the K_m as an apparent affinity since it does not provide a direct measure of the real affinity of the substrate and the kinase (K_d). Adams and colleagues reported that the K_m values obtained in the steady-state kinetic analyses may contain terms related to steps occurring in the central ternary complex. They further explained how fast and favorable phosphoryl transfer can overcome weak interactions between the enzyme and substrate and further increase the apparent affinity in the thermodynamically coupled systems (*24*). Considering this, we examined K_m for cdk5/p25-catalyzed H1P phosphorylation at high Mg^{2+} concentrations. For substrate recognition, K_m includes all the rate constants in the reaction in Scheme 2 as shown below:

$$K_m = (k_{-2} + k_3)k_4/k_2(k_3 + k_4) \quad (16)$$

Since $k_{-2} > k_3 < k_4$, the complex expression of K_m can be simplified into the approximation given by eq 17:

$$K_m = k_{-2}/k_2 \quad (17)$$

That is exactly the same expression for the real substrate affinity K_d. As observed by Adams, we found that the slow phosphoryl transfer of H1P phosphorylation at high Mg^{2+} concentrations ($k_{-2} > k_3 < k_4$) allows a direct measurement of K_d from K_m.

(*ii*) *Proton Transfer and Rate-Limiting Step at Low Mg^{2+} Concentrations*. No SKIE was detected on k_{cat}, k_{cat}/K_{ATP}, or k_{cat}/K_{H1P} at low Mg^{2+} concentrations. The lack of a

SKIE on k_{cat} should be interpreted cautiously, and three mechanisms are possible. First, if the phosphoryl transfer step in the transition state is preceded or followed by a slow conformational change, a small SKIE or no SKIE would be detected for k_{cat}. Second, if the product release step represented as k_4 in Scheme 2 is relatively slow ($k_3 > k_4$), then k_{cat} is approximately equal to k_4 and the observed SKIE would be greatly diminished. Third, if the hydroxyl proton was abstracted after the transfer of the γ-phosphate, a small SKIE or no SKIE would be observed. No special driving force is required for this proton transfer since the pK_a values of the *O*-phosphonothreonine are very low (*29*). This mechanism is not likely, though, because of the SKIE detected on k_{cat} at high Mg^{2+} concentrations (see below). The lack of a SKIE on k_{cat}/K_{ATP} or k_{cat}/K_{H1P} could be interpreted as a slow conformational change associated with the chemical transfer step.

Is There a General Base in the Catalysis? The observation of a large kinetic SKIE on cdk5/p25-catalyzed H1P phosphorylation suggests that the hydroxyl proton was abstracted by a general base in the active site. Indeed, there is structural evidence from the X-ray analysis of members of the cdk family that a conserved aspartate (Asp-127 in cdk2 or Asp-126 in cdk5) is within hydrogen bonding distance of the hydroxyl and, therefore, may serve as a general base catalyst. The dependence of the maximum rate on pH provides additional evidence of a general base catalyst. The pH profile of k_{cat} suggests that a group with a pK_a of 6.1 must be unprotonated for activity. The peptide has no pK values in this pH range, and the pK_a obtained for protonation of the γ-phosphate of ATP is 4.6 (*30*); therefore, the decrease in rate with the change in pH must reflect the titration of enzyme residues. The group with a pK_a of 6.1 is most likely the general base.

An ATPase reaction that is intrinsic to the protein kinase provides an opportunity to estimate pK_a values from different enzyme forms. The pH profiles of k_{cat} and k_{cat}/K_{ATP} of ATPase are bell-shaped (Figure 4). The pK_a of the acidic limb is identical with that obtained from the kinase reaction within experimental error. In addition, since the pK_a of the catalytic base is essentially the same when determined from the ATPase reaction under the condition representing free enzyme (6.5) and from the kinase reaction under the condition representing the E·ATP·H1P complex (6.1), the presence of H1P and ATP in the active site does not affect the pK_a of the base.

The potential role of Asp-126 as a general base raises an interesting question regarding the role of the conserved aspartate in protein kinases. On the basis of available crystal structures, it is very likely that an aspartate residue within hydrogen bonding distance of the hydroxyl of the substrate is conserved in all protein kinases. This aspartate is clearly important for efficient catalysis, since replacement of it with alanine in PKA and PhK decreased k_{cat} by 2−3 orders of magnitude. The role of this conserved aspartate has drawn considerable attention. Although a general acid−base role has been given special consideration in the literature (*29*, *31*−*33*), many studies do not provide convincing evidence of a general base catalyst. Instead, they support a positioning function of the conserved aspartate by attaining the appropriate attack geometry between the hydroxyl group and γ-phosphate of ATP (*29*). Alternatively, the aspartate could facilitate dissociation by repelling the phospho product (*34*). Whether this carboxyl group serves the same function in other protein kinases is still unclear, and further research is needed.

ACKNOWLEDGMENT

We thank Ken Kosik for providing the enzyme for this work.

REFERENCES

1. Baumann, K., Mandelkow, E. M., Biernat, J., Piwnica-Worms, H., and Mandelkow, E. (1993) Abnormal Alzheimer-like phosphorylation of tau-protein by cyclin-dependent kinases cdk2 and cdk5. *FEBS Lett. 336*, 417–424.
2. Flaherty, D. B., Soria, J. P., Tomasiewicz, H. G., and Wood, J. G. (2000) Phosphorylation of human tau protein by microtubule-associated kinases: GSK3β and cdk5 are key participants. *J. Neurosci. Res. 62*, 463–472.
3. Paudel, H. K., Lew, J., Ali, Z., and Wang, J. H. (1993) Brain proline-directed protein kinase phosphorylates tau on sites that are abnormally phosphorylated in tau associated with Alzheimer's paired helical filaments. *J. Biol. Chem. 268*, 23512–23518.
4. Ishiguro, K., Takamatsu, M., Tomizawa, K., Omori, A., Takahashi, M., Arioka, M., Uchida, T., and Imahori, K. (1992) Tau protein kinase I converts normal tau protein into A68-like component of paired helical filaments. *J. Biol. Chem. 267*, 10897–10901.
5. Ishiguro, K., Sato, K., Takamatsu, M., Park, J., Uchida, T., and Imahori, K. (1995) Analysis of phosphorylation of tau with antibodies specific for phosphorylation sites. *Neurosci. Lett. 202*, 81–84.
6. Lew, J., Huang, Q. Q., Qi, Z., Winkfein, R. J., Aebersold, R., Hunt, T., and Wang, J. H. (1994) A brain-specific activator of cyclin-dependent kinase 5. *Nature 371*, 423–426.
7. Tsai, L. H., Delalle, I., Caviness, V. S. J., Chae, T., and Harlow, E. (1994) p35 is a neural-specific regulatory subunit of cyclin-dependent kinase 5. *Nature 371*, 419–423.
8. Liu, M., Choi, S., Cuny, G. D., Ding, K., Dobson, B. C., Glicksman, M. A., Auerbach, K., and Stein, R. L. (2008) Kinetic studies of Cdk5/p25 kinase: Phosphorylation of tau and complex inhibition by two prototype inhibitors. *Biochemistry 47*, 8367–8377.
9. Romani, A., and Scarpa, A. (1992) Regulation of cell magnesium. *Arch. Biochem. Biophys. 298*, 1–12.
10. Bhatnagar, D., Roskoski, R. J., Rosendahl, M. S., and Leonard, N. J. (1983) Adenosine cyclic 3′,5′-monophosphate dependent protein kinase: A new fluorescence displacement titration technique for characterizing the nucleotide binding site on the catalytic subunit. *Biochemistry 22*, 6310–6317.
11. Segel, I. H. (1975) Enzyme Kinetics, John Wiley & Sons, New York.
12. Cook, P. F. (1982) Kinetic studies to determine the mechanism of regulation of bovine liver glutamate dehydrogenase by nucleotide effectors. *Biochemistry 21*, 113–116.
13. Cook, P. F., Neville, M. E. J., Vrana, K. E., Hartl, F. T., and Roskoski, R. J. (1982) Adenosine cyclic 3′,5′-monophosphate dependent protein kinase: Kinetic mechanism for the bovine skeletal muscle catalytic subunit. *Biochemistry 21*, 5794–5799.
14. Gaffney, T. J., and O'Sullivan, W. J. (1964) Kinetic studies of the activation of adenosine triphosphate-lombricine phosphotransferase by magnesium ions. *Biochem. J. 90*, 177–181.
15. Fromm, H. J. (1979) Use of competitive inhibitors to study substrate binding order. *Methods Enzymol. 63*, 467–486.
16. Sun, G., and Budde, R. J. (1997) Requirement for an additional divalent metal cation to activate protein tyrosine kinases. *Biochemistry 36*, 2139–2146.
17. Vicario, P. P., Saperstein, R., and Bennun, A. (1988) Role of divalent metals in the kinetic mechanism of insulin receptor tyrosine kinase. *Arch. Biochem. Biophys. 261*, 336–345.
18. Saylor, P., Wang, C., Hirai, T. J., and Adams, J. A. (1998) A second magnesium ion is critical for ATP binding in the kinase domain of the oncoprotein v-Fps. *Biochemistry 37*, 12624–12630.
19. Armstrong, R. N., Kondo, H., Granot, J., Kaiser, E. T., and Mildvan, A. S. (1979) Magnetic resonance and kinetic studies of the manganese(II) ion and substrate complexes of the catalytic subunit of adenosine 3′,5′-monophosphate dependent protein kinase from bovine heart. *Biochemistry 18*, 1230–1238.
20. Brown, N. R., Noble, M. E., Endicott, J. A., and Johnson, L. N. (1999) The structural basis for specificity of substrate and recruitment peptides for cyclin-dependent kinases. *Nat. Cell Biol. 1*, 438–443.
21. Sun, G., and Budde, R. J. (1997) Requirement for an additional divalent metal cation to activate protein tyrosine kinases. *Biochemistry 36*, 2139–2146.
22. Matte, A., Tari, L. W., Goldie, H., and Delbaere, L. T. (1997) Structure and mechanism of phosphoenolpyruvate carboxykinase. *J. Biol. Chem. 272*, 8105–8108.
23. Lovitt, B., Vanderporten, E. C., Sheng, Z., Zhu, H., Drummond, J., and Liu, Y. (2010) Differential effects of divalent manganese and

magnesium on the kinase activity of leucine-rich repeat kinase 2 (LRRK2). *Biochemistry 49*, 3092–3100.
24. Lieser, S. A., Aubol, B. E., Wong, L., Jennings, P. A., and Adams, J. A. (2005) Coupling phosphoryl transfer and substrate interactions in protein kinases. *Biochim. Biophys. Acta 1754*, 191–199.
25. Schowen, B. K., and Schowen, R. L. (1982) Solvent isotope effects on enzyme systems. *Methods Enzymol. 87*, 551–606.
26. Venkatasubban, K. S., and Schowen, R. L. (1984) The proton inventory technique. *Crit. Rev. Biochem. 17*, 1–44.
27. Stein, R. L. (1985) Transition-state properties for the association of α-1-protease inhibitor with porcine pancreatic elastase. *J. Am. Chem. Soc. 107*, 6039–6042.
28. Cleland, W. W. (1975) Partition analysis and the concept of net rate constants as tools in enzyme kinetics. *Biochemistry 14*, 3220–3224.
29. Zhou, J., and Adams, J. A. (1997) Is there a catalytic base in the active site of cAMP-dependent protein kinase? *Biochemistry 36*, 2977–2984.
30. Martell, A. E., and Smith, R. M. (1982) Critical Stability Constants, Vol. *5*, Plenum Press, New York.
31. Yoon, M. Y., and Cook, P. F. (1987) Chemical mechanism of the adenosine cyclic 3′,5′-monophosphate dependent protein kinase from pH studies. *Biochemistry 26*, 4118–4125.
32. Ward, W. H., Cook, P. N., Slater, A. M., Davies, D. H., Holdgate, G. A., and Green, L. R. (1994) Epidermal growth factor receptor tyrosine kinase. Investigation of catalytic mechanism, structure-based searching and discovery of a potent inhibitor. *Biochem. Pharmacol. 48*, 659–666.
33. Adams, J. A. (1996) Insight into tyrosine phosphorylation in v-Fps using proton inventory techniques. *Biochemistry 35*, 10949–10956.
34. Madhusudan, Trafny, E. A., Xuong, N. H., Adams, J. A., Ten Eyck, L. F., Taylor, S. S., and Sowadski, J. M. (1994) cAMP-dependent protein kinase: Crystallographic insights into substrate recognition and phosphotransfer. *Protein Sci. 3*, 176–187.